MEASUREMENTS OF FIELD STABILITY AGAINST PERTURBATIONS IN NON-UNIFORM LINAC STRUCTURES

G. Dôme and I. White

European Organization for Nuclear Research (CERN),
Geneva, Switzerland

Summary

Scale models of tank 1 (0.75 - 5 MeV) and tank 2 (10 - 30 MeV) have been used to investigate the stability of the axial electric field against individual cell tuning errors.

As reported previously [1], a compensated structure for tank 1 consists of two stems at 45° on each drift tube, alternating at 180° from one drift tube to the next. The axial electric field is shown to be unaffected by a perturbation produced by a metallic rod parallel to the axis and placed at one end of the tank. Insensitivity of the field to perturbations has also been achieved experimentally with two stems at 150° on each drift tube, all stems being parallel from one drift tube to the next. The frequency shift of the Alvarez zero-mode due to the stems is larger than predicted by theory in tank 1.

A compensated structure for tank 2 is the cross-bar with an appropriate stem diameter. When the stem diameter is kept constant throughout the tank, compensation is achieved only on the average and the axial field is strongly affected in the region where the perturbation is introduced. This effect can be reduced by compensating locally small groups of drift tubes; a good stability of the field is then obtained. The frequency shift of the Alvarez zero-mode due to the stems is close to the theoretical value in tank 2.

Finally, a full scale 200 MHz cross-bar cell designed to accelerate protons at 140 MeV in the π mode (defined as the phase-shift over a complete geometrical period) of the stem passband has been tested at a power level of 435 kW, which would produce an acceleration rate of 4 MeV/m at $\varphi_s = 0$, with an average axial field of 4.6 MV/m.

Measurements on Tank 1 model (0.75 - 5 MeV)

With a reduction factor of 0.1900 this model is scaled from the first 25 cells of the new 20 MeV linac injector at Saclay. Previous work [1] has shown that the structure can be compensated, i.e. the passband associated with the stems can be joined to the E01 passband, by a stem arrangement consisting of two stems at 135° on each drift tube, alternating at 180° from one drift tube to the next. Confirming the theoretical expectation [1], figure 1 shows that the same result can be achieved with an angle of 45° between the stems. This latter configuration has been chosen for field measurements as it is believed to be mechanically more practical.

Figure 2 shows that with this arrangement the axial electric field is remarkably insensitive to a frequency perturbation introduced at the output end of the tank. In this graph, the ordinate chosen is a cell averaged field defined as (peak frequency perturbation in kHz)$^{1/2}$ x gap/length of the cell. This formula roughly converts the peak field in a gap, which is the only quantity measurable with some accuracy on small scale models, into an approximate average field which is more uniform throughout the tank. The perturbing body used was a metallic bead of 3 mm diameter.

The electric field on the axis was measured by a standard frequency perturbation technique. The tank was made to oscillate on its resonant frequency by being part of a closed amplification loop. With this method, the input and output couplings must be as weak as can be tolerated for oscillation to occur; large couplings lower the loaded Q of the tank, and the measured shifts in the oscillating frequency of the closed amplification loop are then smaller than the actual resonant frequency shifts of the unloaded tank [2].

No attempt in this and similar subsequent graphs has been made to smooth out errors due to inaccurate drift tube assembly. Such errors appear as undulations on the electric field distribution (see figure 2, and figures 4 to 8).

For low energy cells, compensation depends essentially on the angle between the stems and not on their diameter [1]. Therefore even with a constant stem diameter throughout the tank, the structure of figure 2 is almost locally compensated, which accounts for its good stability against perturbations.

The appropriate angle between the stems for compensation of tank 1 model is about 135°, with stems alternating at 180° from one drift tube to the next in order to prevent the occurrence of any angle larger than 135° between the projections of the stems on a tank cross-section. As explained earlier [1], a larger angle would involve a zero-mode stem resonance which would be lower in frequency than the zero-mode of the E01 passband; consequently the two passbands could not join.

Nevertheless, a structure with two stems at an angle ϕ (< 180°) on each drift tube, all stems being parallel from one drift tube to the next, produces this angle of ϕ as well as the larger angle (360°-ϕ) between the stems. Therefore, such structures have been investigated systematically, with the angle ϕ varying from 90° to 180° by steps of 15°. Figure 3 shows the corresponding dispersion curves around the zero-modes, while the main features are summarized in Table I.

The theoretical zero-mode frequency for the stem passband has been deduced from figure 4 in reference [1]. In all cases the experimental zero-mode frequency of the stem passband appears to correspond to the larger angle (360° - ϕ) between the stems; there is no evidence that a second stem passband corresponding to the smaller angle ϕ exists. As a consequence, full compensation is not possible since the zero-mode of the stem passband is always lower in frequency than the zero-mode of the E01 passband.

For angles of ϕ between 135° and 180°, the E01 passband is practically the same as when the stems alternate by 180° from one drift tube to the next (see figures 1 and 3). Thus with ϕ = 135° it might be expected, on the ground of the large mode spacing, that the axial electric field would be insensitive to perturbations. Figure 6 shows quite clearly that this is not the case: in fact, this structure is the most sensitive to perturbations.

TABLE I

Comparison of structures with two stems per drift tube, all stems being parallel along the tank

ϕ (degrees)	f_o (MHz)	$f_1 - f_o$ (MHz)	Extrapolated 0 mode of the measured stem passband (MHz)	Theoretical 0 mode of the stem passband, corresponding to an angle (360° - ϕ) (MHz)
180	1052.99	72.43	895	869
165	1053.49	77.08	840	810
150	1053.19	90.92	777	759
135	1052.79	130.64	722	714
120	1053.30	15.04	710	673
105	1053.05	23.20	665	638
90	1052.20	28.28	640	605
0	1050.11	32.10	480	462

f_o = zero-mode frequency of the E_{01} passband

f_1 = $\pi/25$ mode frequency of the E_{01} passband

Important remark: for ϕ = 0, there is only one stem per drift tube.

Figure 3 emphasizes an important discontinuity in the shape of the E01 passband for a value of ϕ between 135° and 120°. Although this seems to be connected with the angle of 135°, no explanation has yet been found for this phenomenon.

Field measurements on structures with stem angles of 120°, 150° and 180° are shown in figures 5, 7, 8. The least sensitive to perturbations is the structure with $\phi = 150^\circ$, but the electric field in the simple structure with $\phi = 180^\circ$ also appears quite stable. For comparison, the field stability against perturbation in the Saclay structure is shown in figure 4. This structure has only one stem per drift tube, all stems being parallel.

A structure which is locally compensated throughout its length, is extremely insensitive to manufacturing errors and is thus expected to produce the theoretical field which is computed for a perfect structure. Therefore, the peak axial electric field measured in the best compensated structures for tank 1 (fig. 2 and fig. 7) has been compared in figure 9 with values of the field in the centre of the gaps, derived from recent numerical computations [3]. The theoretical variation of electric field along the non-uniform structure was obtained by matching the computed maximum currents in the outer walls of two adjacent cells [5]. The splitting of the theoretical curve into three parts marked with A, B, C corresponds to a change of the drift tube bore diameter from A to B, and of the drift tube outer diameter from B to C.

Both computed and measured fields are referred to the average field in the first cell. Since the measured field is referred absolutely to the square root of the total energy stored in the tank, the scale for the measured field has been determined by using the theoretical ratio of (total stored energy in all cells)/(average field in the first cell)^2, obtained from the numerical computations of Alvarez cells. The agreement between theoretical and measured fields is as good as may be expected from the mechanical accuracy of the model; in fact, the difference between the measurements made on the two types of compensated structures for tank 1 shows the magnitude of the experimental errors. The computed resonant frequency of the individual cells in the Alvarez 0 mode, taking into account the stem frequency shifts (see for example reference 6), is constant within 0.1% along the tank.

The theoretical frequency shift of the E010 mode due to the stems at 1053 MHz has been computed as 0.69 MHz per stem for the average cell of tank 1 model, the stem diameter being 5 mm [3 and 4]. In fact, this frequency shift decreases steadily from 0.77 MHz to 0.62 MHz per stem along the tank. Figure 19a gives a survey of all the points which have been measured for various stem configurations. It shows that the experimental frequency shift is greater than expected theoretically, although the large frequency dispersion for two stems per drift tube has not yet been investigated. From Table I it seems that the measured frequency shift due to a second stem varies between 2 and 3 MHz, depending on the angle between the two stems.

Measurements on Tank 2 model (10 - 30 MeV)

With a reduction factor of 0.1618 this model is scaled from tank 2 of the CERN linac injector. A compensated structure for this tank is the cross-bar with an appropriate stem diameter [1]. The values of stem diameter required for local compensation have been derived theoretically from figure 12 in reference 1; they are plotted in figure 17.

Figure 11 shows dispersion curves around the zero-mode for constant stem diameters of 6.16 mm, 10 mm, 12 mm and one for a variable stem diameter in a structure which has been compensated locally and will be described later (in figure 16). A stem diameter of 10 mm appears to be slightly overcompensated, which is consistent with the theoretical value (for an average cell) of 9.71 mm derived from figure 17. As already pointed out in our earlier paper [1], the strange curvature of the E01 passband is due to the fact that with a constant stem diameter, part of the tank is cut off around the zero-mode. The dispersion curve for the locally compensated structure shows extremely good continuity at zero-mode: the E01 and the stem passbands then join without a stopband all along the structure, and no part of the tank is cut off in the neighbouring modes.

The stem arrangement for the scale model of the actual CERN linac consists of two stems of diameter 6.16 mm at 90° on each drift tube, all stems being parallel from one drift tube to the next. The tilt produced on the field by a perturbation at the output end of the tank, figure 10, is quite remarkable. In this tank also, an averaged field was computed as (peak frequency perturbation in kHz)$^{1/2}$ x gap/length of the cell. The perturbing body used was a dielectric bead of diameter 5.1 mm and relative dielectric constant of 5.81. For this and for following graphs of a similar nature, the resonant frequency of each cell in the Alvarez 0 mode has been computed theoretically, allowance being made for the stem frequency shifts [3]. The frequency drop in the end cells is merely due to the fact that the end plates have not been fitted with half-stems. The discrepancy of 3.5 MHz between the theoretical and measured Alvarez frequencies for our tank 2 model can be attributed to manufacturing errors.

In a cross-bar structure of constant diameter, compensation can only be achieved on the average. With a stem diameter of 10 mm, figure 12 shows that the field is strongly affected in the neighbourhood of the perturbation. Improvement can be gained by compensating on the average small groups of drift tubes. Even with five groups of constant stem diameter, the compensation is not sufficient as shown in figure 14. It is thus absolutely necessary to compensate locally.

Figures 13 and 14 show that an abrupt change in the resonant frequency of adjacent cells results in the slope of the electric field along the axis being discontinuous at that point.

Field measurements shown in figure 15 were carried out with the theoretical values of stem diameter required for local compensation, rounded off to the nearest millimetre. While the results with these "theoretical" values are rather good, even better field stabilization was obtained when the stem diameters on the various drift tubes were optimized experimentally, yielding the results of figure 16. It is remarkable that the stability of the field has been closely achieved even though the resonant frequencies of individual cells exhibit a large variation throughout the tank (due to the increasing stem diameters used for compensation). A comparison between the theoretical values of stem diameter and those found by experimental optimization is shown in figure 17. Considering that the theory applies basically to square waveguides without drift tubes [7], the agreement is quite remarkable.

The technique for achieving good compensation is of interest: it consisted of examining the axial field patterns of the modes adjacent to the zero-mode, seeing which sections of the tank were cut off, then making corrections to the stem diameters. For perfect compensation, no part of the tank should be cut off in the neighbourhood of the zero-mode of the E01 passband.

As for tank 1, the fields in the centre of the gaps, measured on the axis in the best locally compensated structure for tank 2 (figure 16), have been compared in figure 18 with those derived from recent numerical computations [3]. The agreement is still quite good if it is taken into account that the model has not been perfectly compensated and moreover that the individual cell frequencies show up a large detuning. (The field perturbations due to tuning errors in a compensated structure are zero only up to the first order in these tuning errors.) The theoretical variation of electric field along the non-uniform structure has again been obtained by matching the computed maximum currents in the outer walls of two adjacent cells. For tank 2 this matching condition results in the average electric field on the axis being constant within 0.45% along the tank.

In all the previous measurements, the overall frequency of the tank was lowered by the perturbing rod. In order to suppress any possible effect of this overall frequency shift, the half drift tubes on the end plates were shortened (one at a time), thereby producing an increase in the overall frequency of the tank. The metallic rod was then also introduced by an amount just sufficient to bring the tank frequency back to its original value. Such measurements have shown that the field amplitude variations due to both perturbing effects essentially add together.

Finally, the theoretical frequency shift of the E010 mode due to the stems at 1252 MHz has been computed to be 7.8 MHz/(cm^2 of total stem cross-sectional area) for the average cell in tank 2 model [3 and 4]. This frequency shift decreases steadily from 8.7 MHz/cm^2 to 7.3 MHz/cm^2 along the tank. Figure 19b gives a survey of all the experimental points which have been obtained for various numbers of stems per drift tube, stem configurations and stem diameters, the stem diameter being constant throughout the tank. All these data are consistent with a frequency shift of 6.3 MHz/cm^2, which is slightly smaller than the theoretical value.

High Power Test of Cross-bar Cavity

Theory and low power measurements have shown that above 100 MeV the cross-bar structure operating in the π mode of the stem passband would have a higher shunt impedance than the Alvarez structure operating in 0 mode [8]. As well as providing information on the power handling capabilities of the former structure, a full scale model would highlight any constructional difficulties which would be encountered in a full scale linac. Consequently a 200 MHz cross-bar cell consisting of one full drift tube and two half drift tubes, designed to accelerate protons at 140 MeV, was constructed. The dimensional information on the cavity is:

Diameter of cell	66.0 cm
Length of cell	37.00 cm
Diameter of large stems	9.00 cm
Diameter of thin stems	3.80 cm
Length of long drift tube	20.20 cm
Length of short drift tube	3.80 cm
Diameter of drift tubes	12.00 cm
Drift tube profile outer radius	3.30 cm
Drift tube profile inner radius	0.95 cm
Drift tube bore diameter	3.50 cm

Low power measurements of frequency and unloaded Q are compared with their design values in Table II.

TABLE II

Cross-bar cell for a proton energy of 140 MeV, π mode.

	Design	Model
Resonant frequency	200.00 MHz	200.99 MHz at 20°C
Unloaded Q-factor	17,960	16,560

Theory shows that a resistance of 2.12 mΩ at the foot of each large stem is sufficient to reduce the Q-factor to 12,000.

This model has been tested at a power level of 435 kW without breakdown occurring in the cavity. This power level produces a peak field on the drift tubes of 19.5 MV/m and an acceleration rate of 4 MeV/m at $\varphi_s = 0$, with an average axial field of 4.6 MV/m. Breakdown of the ceramic window in the input coupling loop [9], which was designed for 200 kW, prevented a further increase in the power level.

Good contact between the foot of the large stems and the body of the cavity was essential as these stems carry a peak current of 10,000 Amps at this power level. This appeared to be the only mechanical problem; it was solved so far by spring finger contacts of silver plated bronze berrylium.

Conclusions

When a structure is compensated there is little change in the axial field due to perturbations and manufacturing errors. The reported measurements have shown that the field in a compensated structure is very close to theoretical even with large tuning errors in individual cells. This fact allows the design of future linacs to be entirely based on theoretical fields, with the confidence that these fields would be realized in practice. The field tuners would be ineffective in a compensated structure but they will no longer be needed. Only an overall frequency tuner will still be necessary.

Finally, the cross-bar structure operating in the π mode of the stem passband has proved able to stand fields which are at least as high as those normally used so far in proton linacs.

Acknowledgements

We would like to thank Mr. A. Bellanger for carrying out the low and high power measurements reported in this paper. The construction and design of the high power cross-bar cavity was the work of many people in the ISR 300 GeV Linac Group; special mention should be made of Mr. J. Delfosse for directing the mechanical construction. The power source needed for tests was made available by the MPS Linac Group.

References

1. G. Dôme and I. White, A general theory of multistem drift tube structures proposed for proton linacs, Proceedings of the VI International Conference on High Energy Accelerators, Cambridge, Mass., September 1967 (CEAL-2000, December 1967), p. A-19.

2. H. Hahn and H.J. Halama, Perturbation Measurements of Transverse R/Q in Iris Loaded Waveguides, IEEE Transactions on Microwave Theory and Techniques, Vol. MTT-16, January 1968, p. 22.

3. M. Martini and D.J. Warner, An improved method for calculating proton linac cavities, Paper presented to this Conference, and private communication.

4. M. Bell, private communication.

5. G. Dôme and P. Lapostolle, Sur la distribution des champs dans une longue cavité d'accélérateur de type Alvarez avec et sans compensation, CERN Internal Report ISR-300/LI/68-2, January 1968.

6. G. Parzen, Perturbations and tolerances in a 200 MeV proton linac, Proceedings of the VI International Conference on High Energy Accelerators, Cambridge, Mass., September 1967 (CEAL-2000, December 1967), p. A-34.

7. G. Dôme, Rod loaded waveguides, to be published.

8. A. Carne, G. Dôme, N. Fewell and W. Jüngst, Development of the cross-bar structure for a proton linear accelerator, Proceedings of the V International Conference on High Energy Accelerators, Frascati, September 1965 (CNEN, Rome, 1966), p. 624.

9. P. Bramham, A matched vacuum window for a coaxial line, CERN Internal Report ISR-300/LI/67-54, 1967.

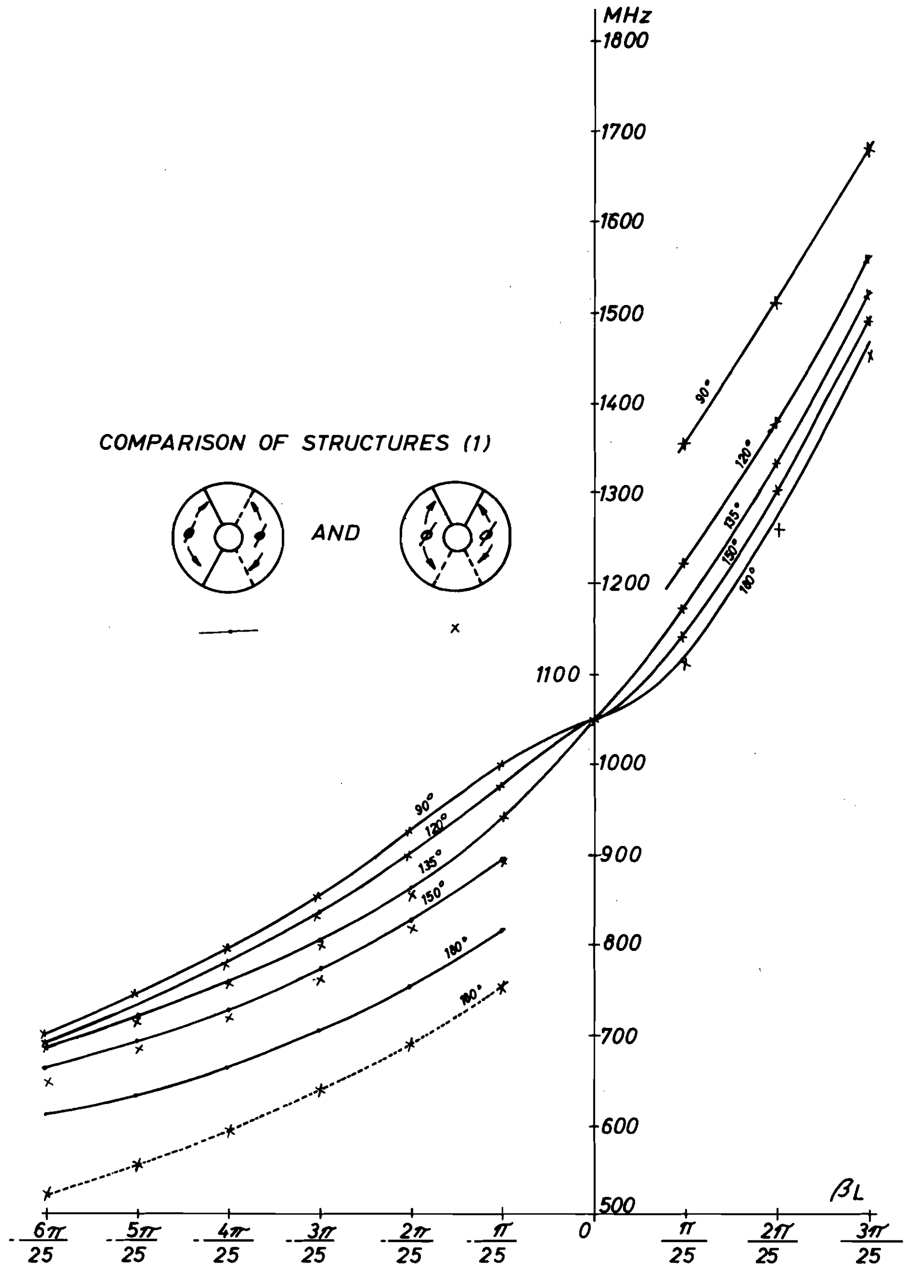

Fig. 1. Dispersion curves of tank 1 model with alternate stems.

(1) ——— stems on even drift tubes

\- - - stems on odd drift tubes.

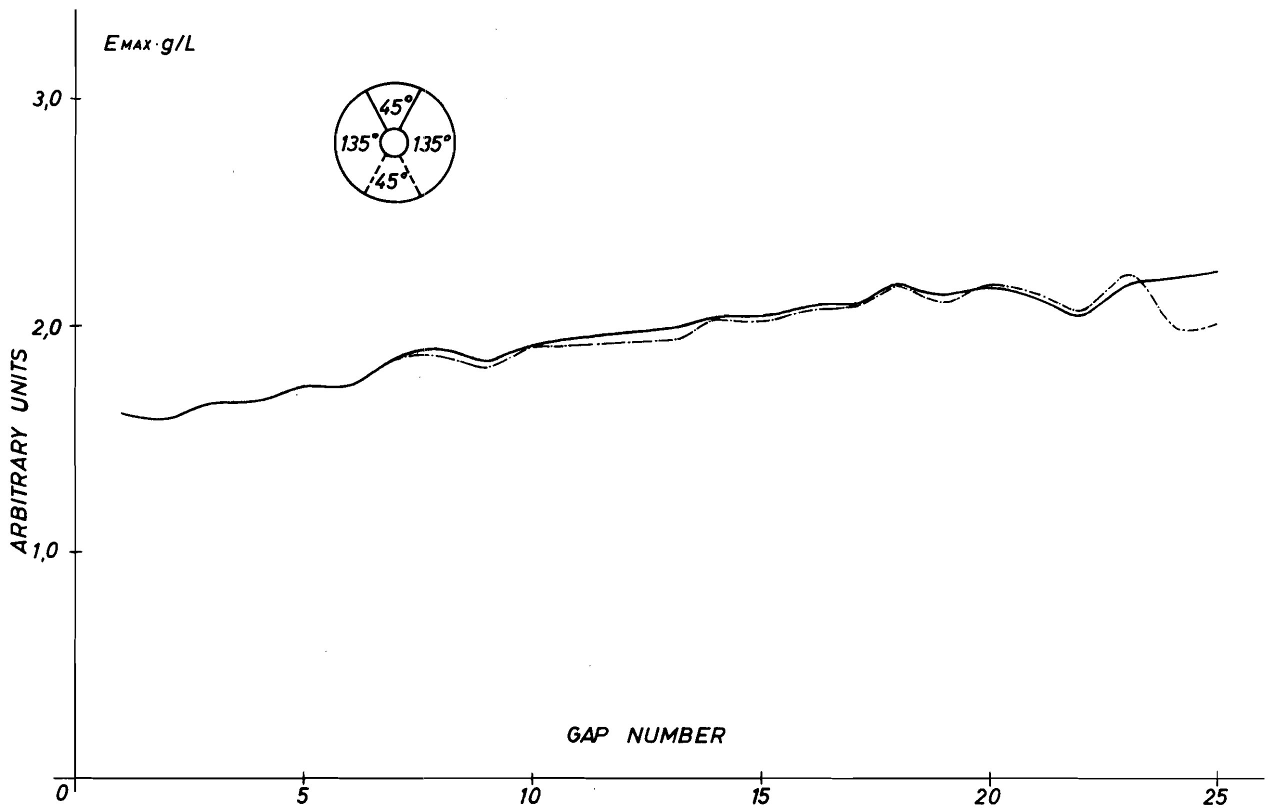

Fig. 2. Field stability against perturbation for tank 1 model. Compensated structure
——— without perturbation (frequency: 1052.69 MHz)
-.-.-. with a tank perturbation of - 4 MHz in cell 25.

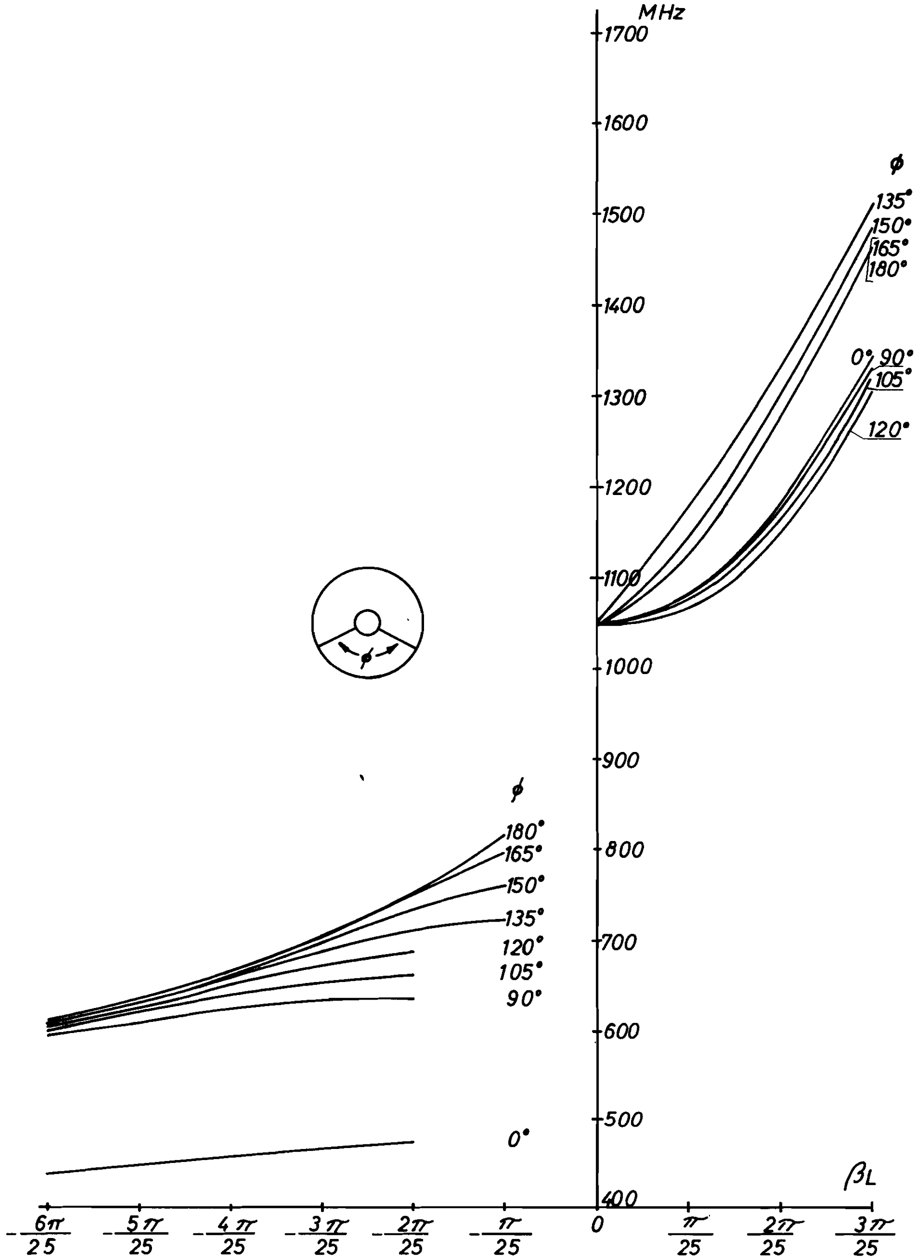

Fig. 3. Dispersion curves for tank 1 model. Parallel stems.

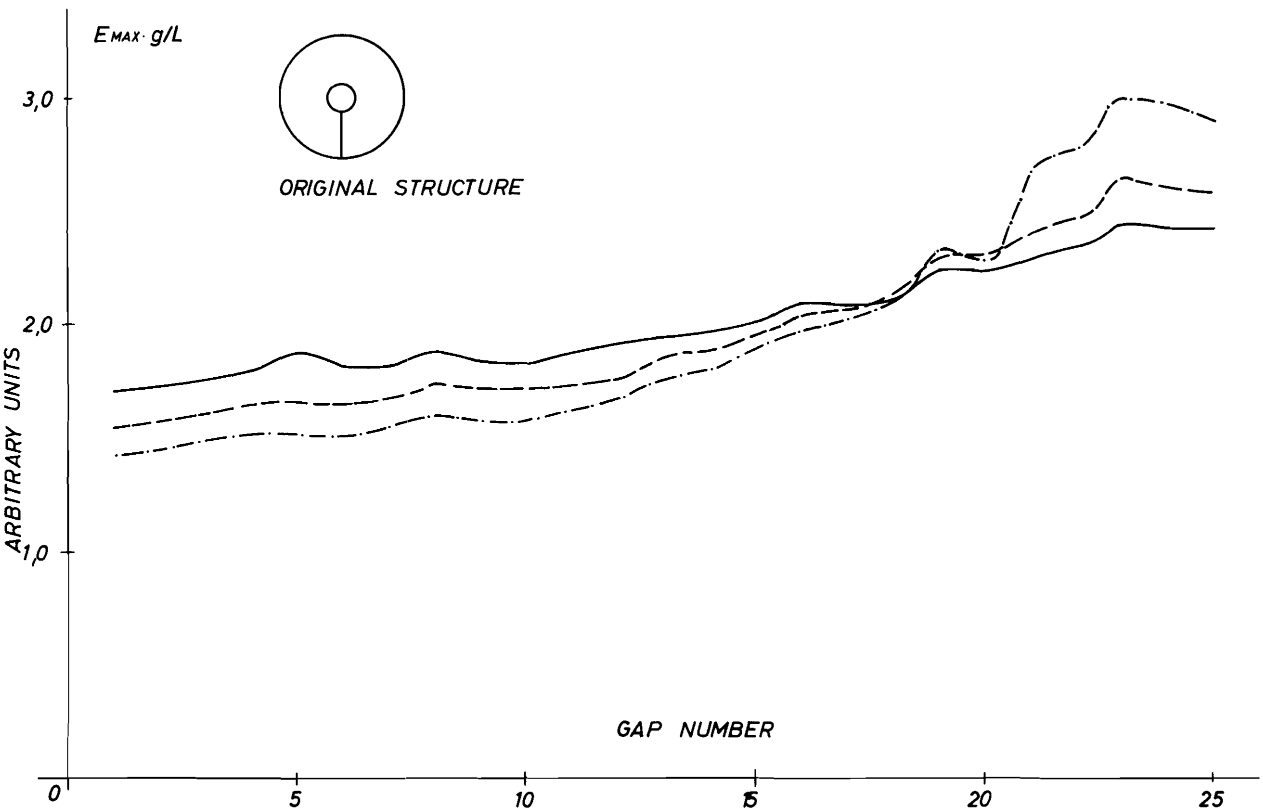

Fig. 4. Field stability against perturbation for tank 1 model. $\phi = 0^{\circ}$.

——— without perturbation (frequency: 1050.90 MHz)
- - - with a tank perturbation of - 2 MHz in cell 25
-.-.-. with a tank perturbation of - 4 MHz in cell 25.

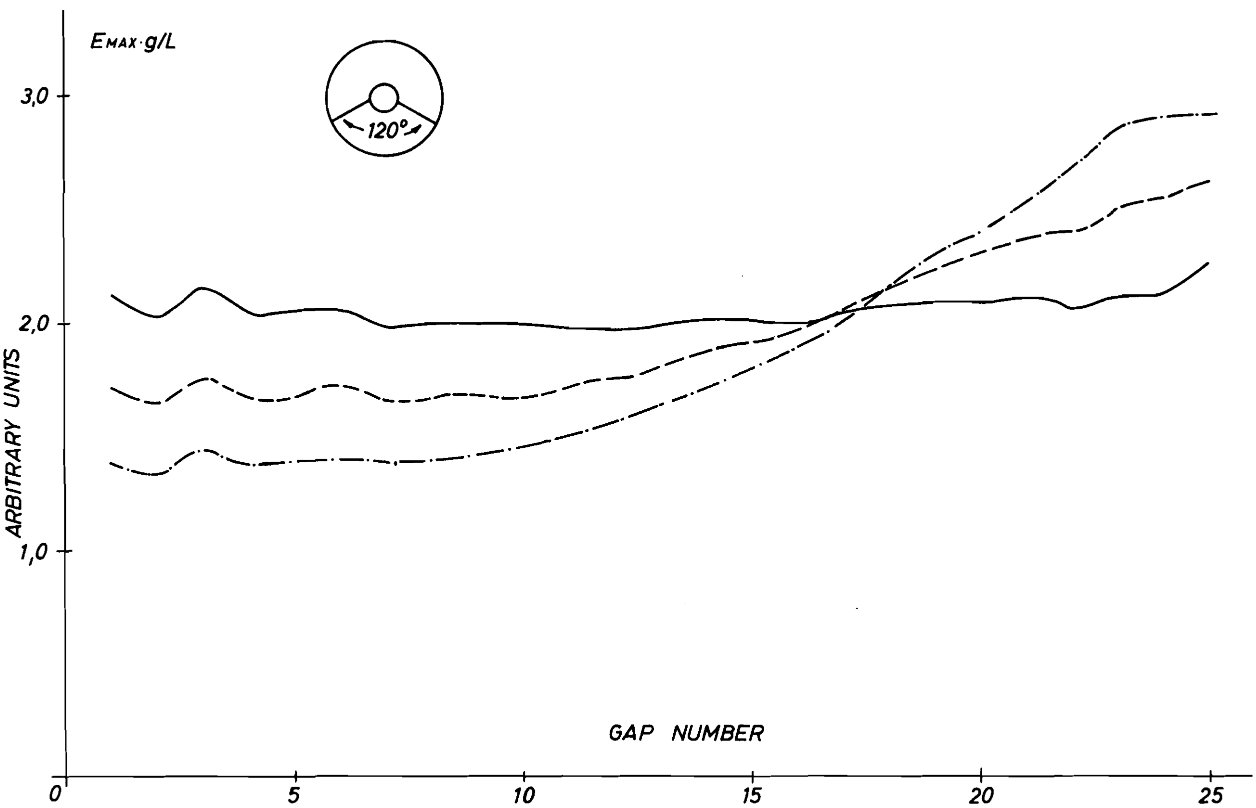

Fig. 5. Field stability against perturbation for tank 1 model. ϕ = 120°.

——— without perturbation (frequency: 1053.30 MHz)
- - - with a tank perturbation of - 2 MHz in cell 25
-.-.-. with a tank perturbation of - 4 MHz in cell 25.

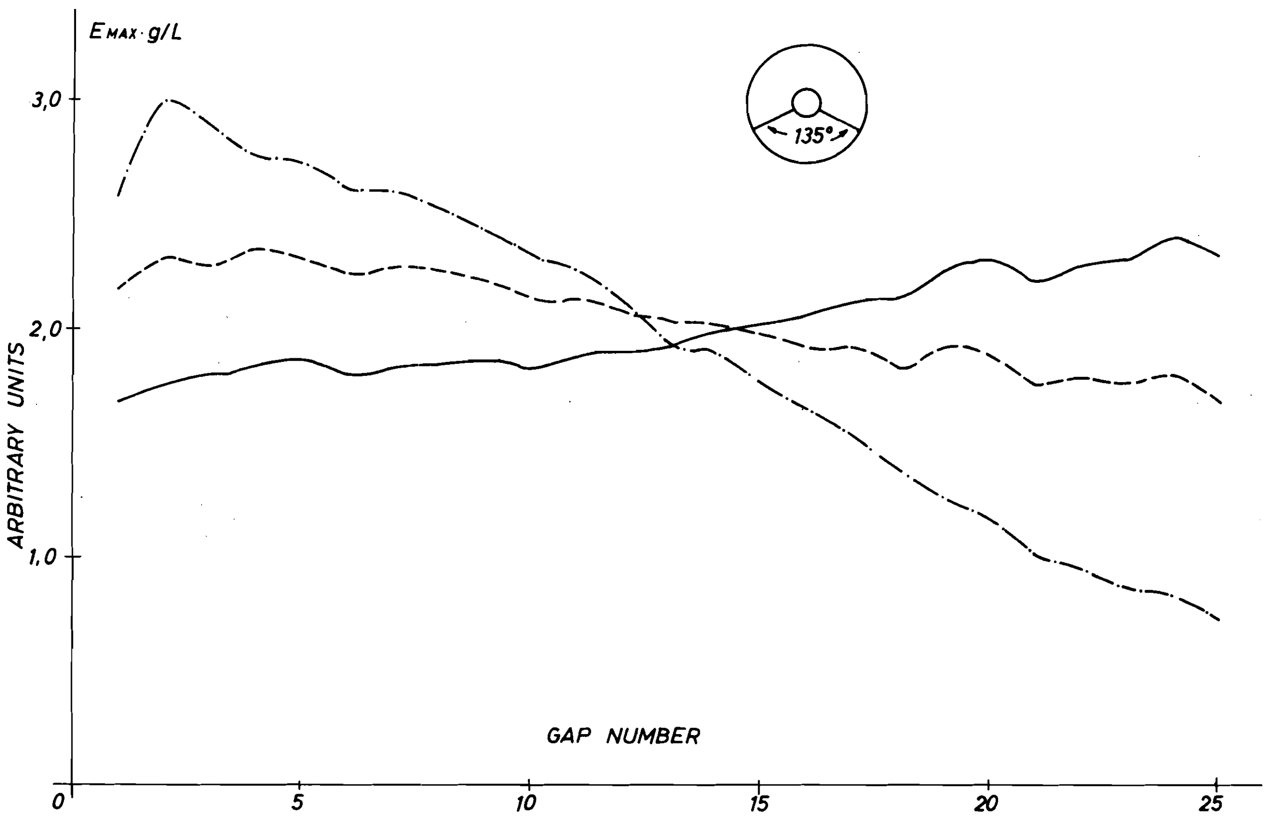

Fig. 6. Field stability against perturbation for tank 1 model. ϕ = 135°.

——— without perturbation (frequency: 1050.79 MHz)

- - - with a tank perturbation of - 2 MHz in cell 25

-.-.-. with a tank perturbation of - 4 MHz in cell 25.

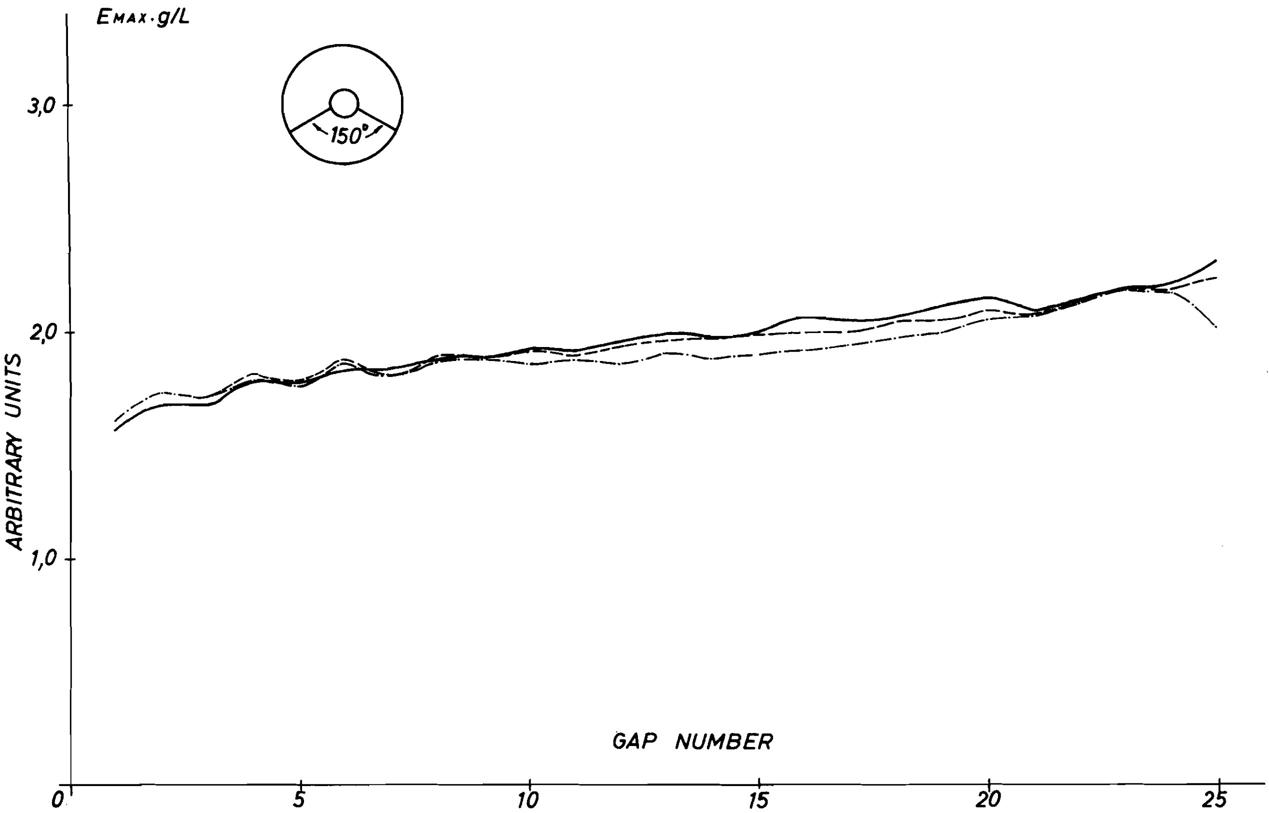

Fig. 7. Field stability against perturbation for tank 1 model. ∅ = 150°.

——— without perturbation (frequency: 1053.19 MHz)
- - - with a tank perturbation of - 2 MHz in cell 25
-.-.-. with a tank perturbation of - 4 MHz in cell 25.

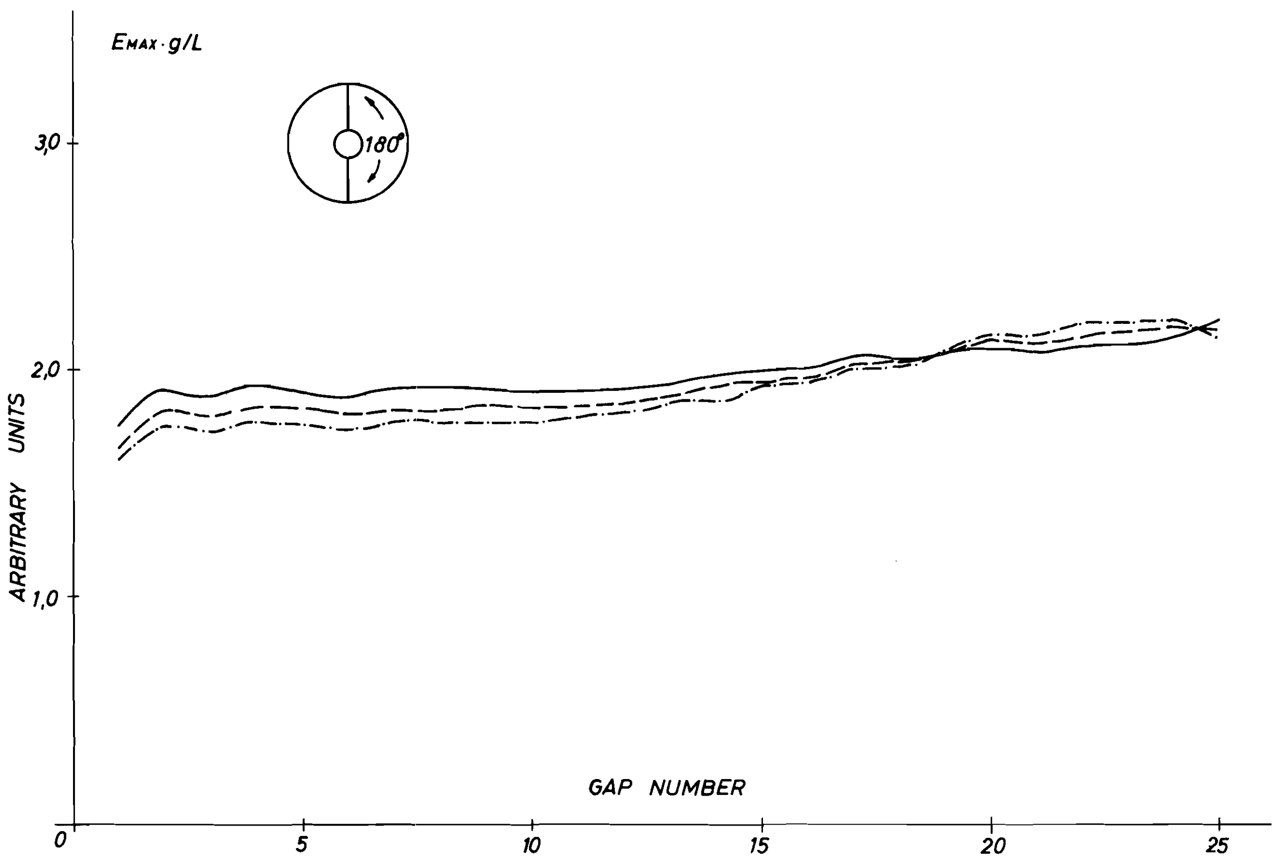

Fig. 8. Field stability against perturbation for tank 1 model. $\phi = 180^{\circ}$.

——— without perturbation (frequency: 1052.99 MHz)
\- - - with a tank perturbation of - 2 MHz in cell 25
-.-.-. with a tank perturbation of - 4 MHz in cell 25.

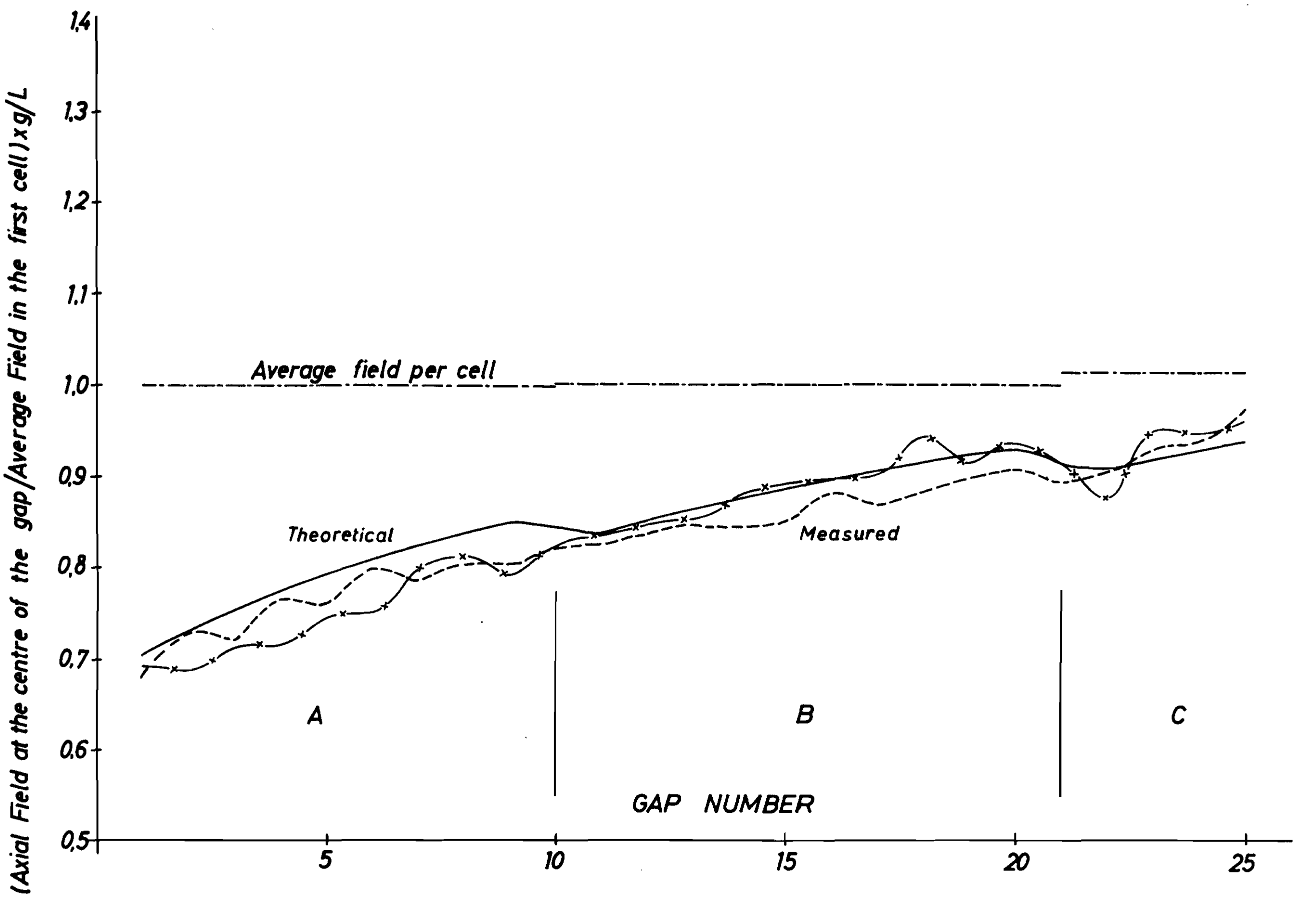

Fig. 9. Comparison of theoretical and measured electric field at the centre of the gaps, for the two best compensated tank 1 models.

——— theoretical field
-x-x-x field measured with two stems at 45°, alternating at 180° from one drift tube to the next (structure of fig. 2)
- - - field measured with two stems at 150°, all parallel (structure of fig. 7).

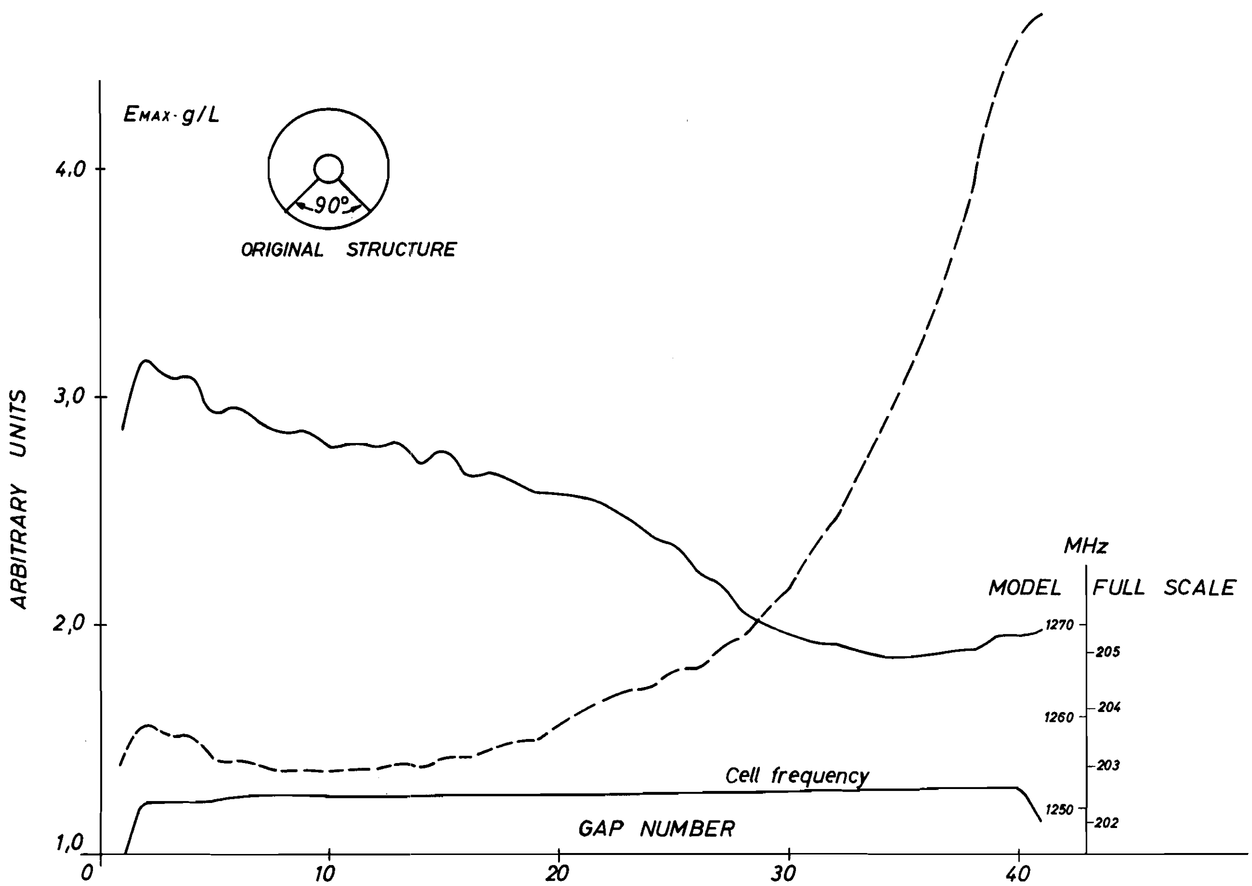

Fig. 10. Field stability against perturbation and resonant frequency of individual cells in the Alvarez mode, for tank 2 model. Original structure, with d_s = 6.16 mm.

——— without perturbation (frequency: 1248.10 MHz)

- - - with a tank perturbation of - 1 MHz in cell 41.

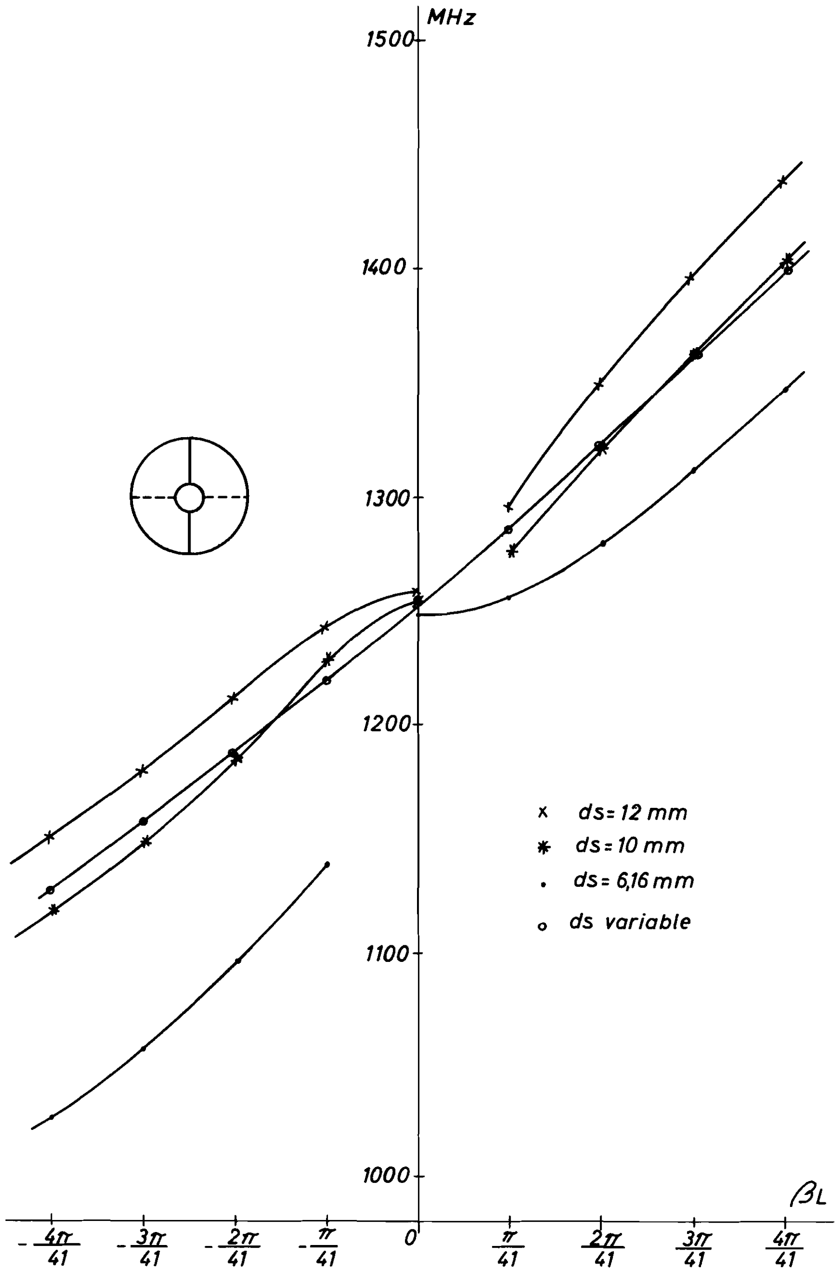

Fig. 11. Dispersion curves of tank 2 model. Cross-bar structure around 0 mode. For the compensated structure d_s is variable from 5 mm to 17 mm.

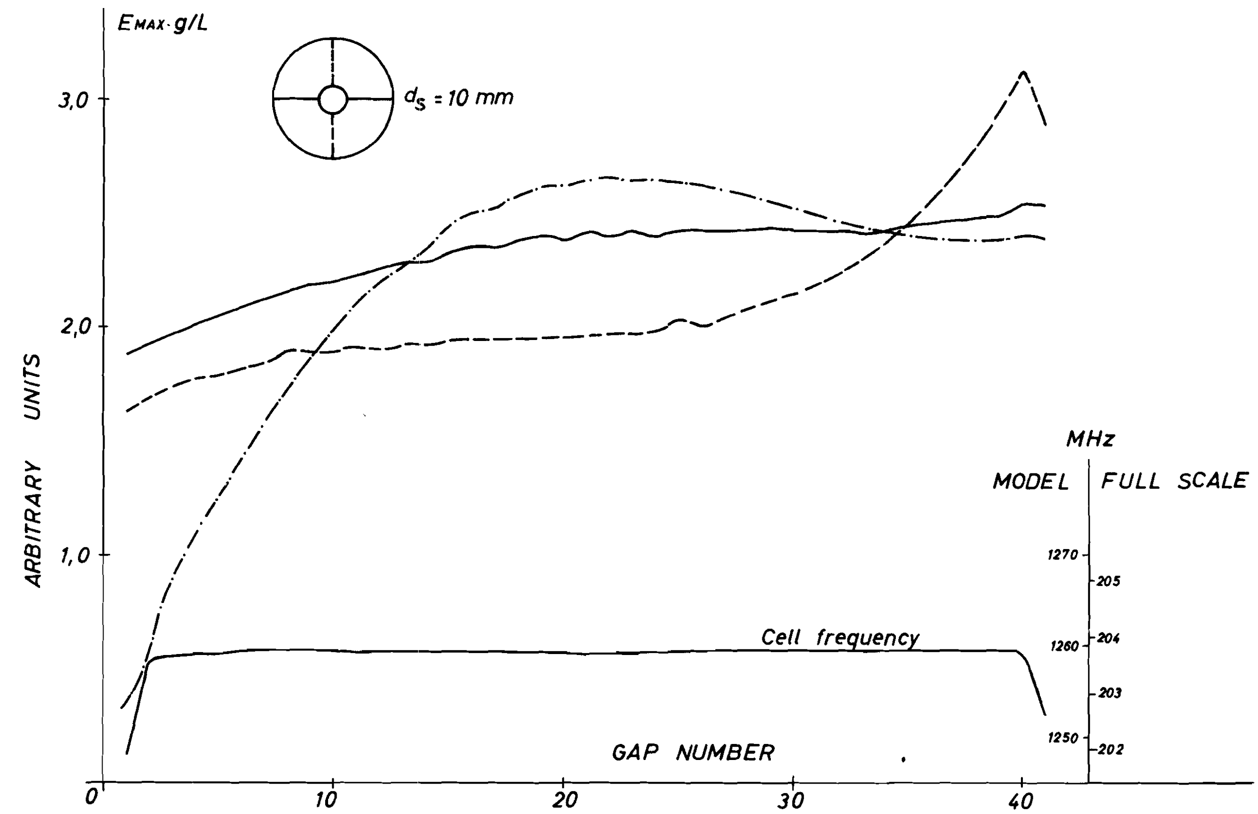

Fig. 12. Field stability against perturbation and resonant frequency of individual cells in the Alvarez mode, for tank 2 model. Cross-bar structure, compensated on the average. Constant d_s = 10 mm.

——— without perturbation (frequency: 1254.39 MHz)
\- - - with a tank perturbation of - 2 MHz in cell 41
-.-.-. with a tank perturbation of - 2 MHz in cell 1.

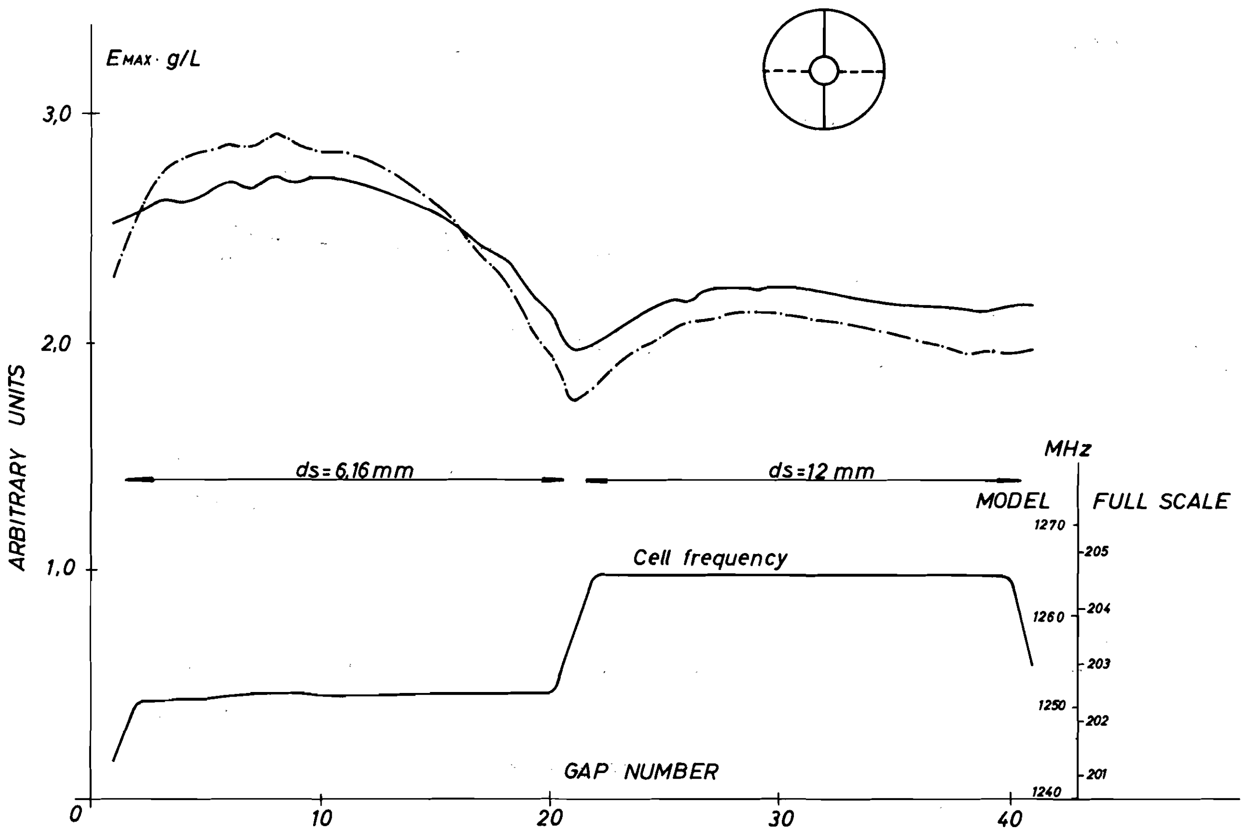

Fig. 13. Field stability against perturbation and resonant frequency of individual cells in the Alvarez mode, for tank 2 model. Effect of a frequency discontinuity on the field.

——— without perturbation (frequency: 1253.54 MHz)

-.-.-. with a tank perturbation of - 2 MHz in cell 1.

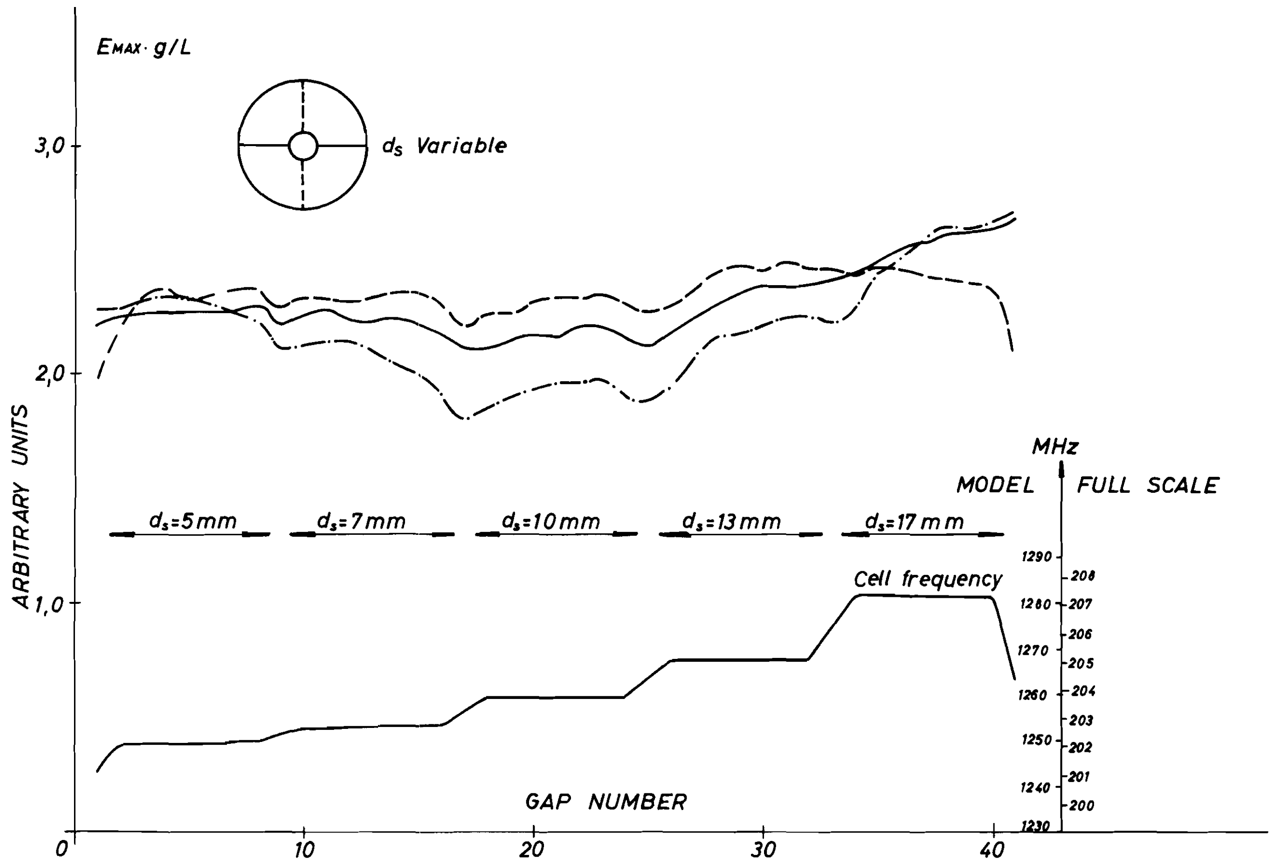

Fig. 14. Field stability against perturbation and resonant frequency of the individual cells in the Alvarez mode, for tank 2 model. Cross-bar structure, compensated in groups of 8 drift tubes.

——— without perturbation (frequency: 1257.79 MHz)

- - - with a tank perturbation of - 2 MHz in cell 41

-.-.-. with a tank perturbation of - 2 MHz in cell 1.

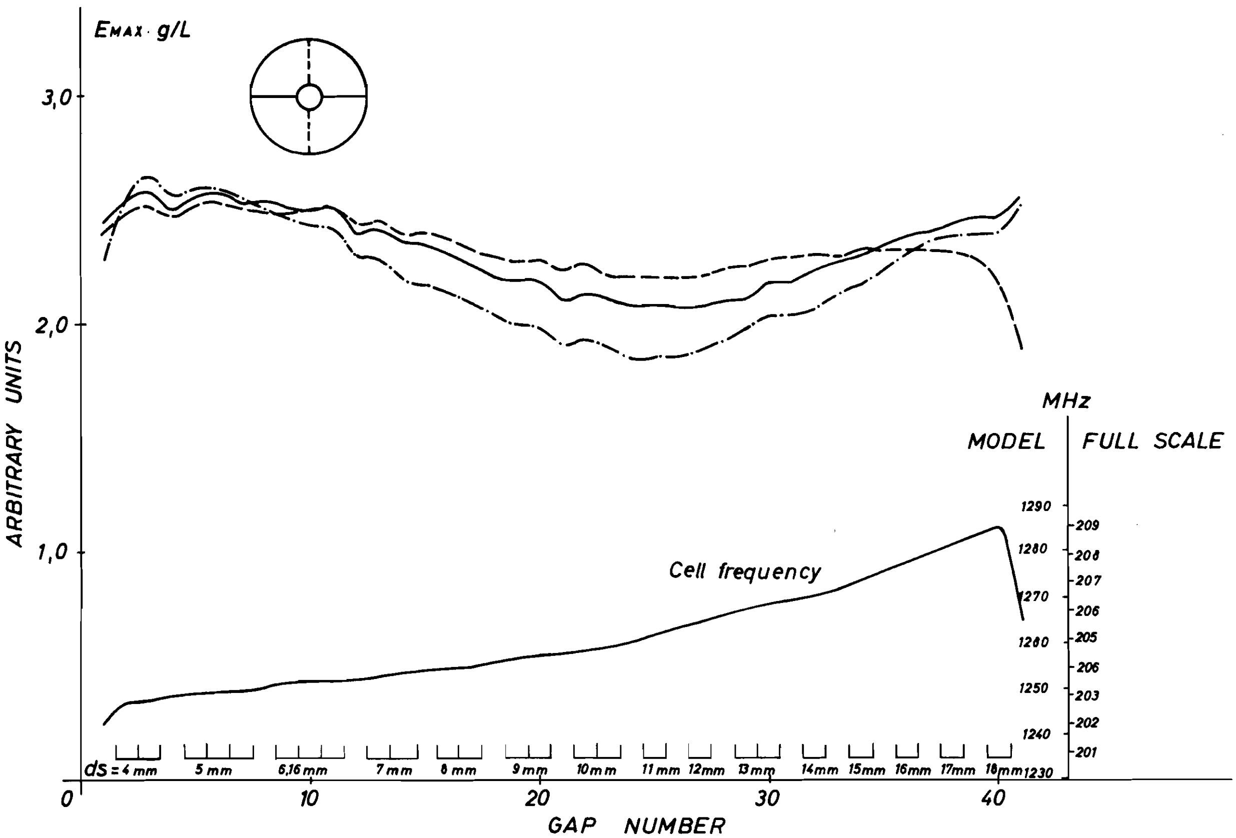

Fig. 15. Field stability against perturbation and resonant frequency of the individual cells in the Alvarez mode, for tank 2 model. Structure compensated locally, with stem diameter d_s adjusted to theoretical values rounded off to the nearest mm.

——— without perturbation (frequency: 1256.49 MHz)
- - - with a tank perturbation of - 2 MHz in cell 41
-.-.-. with a tank perturbation of - 2 MHz in cell 1.

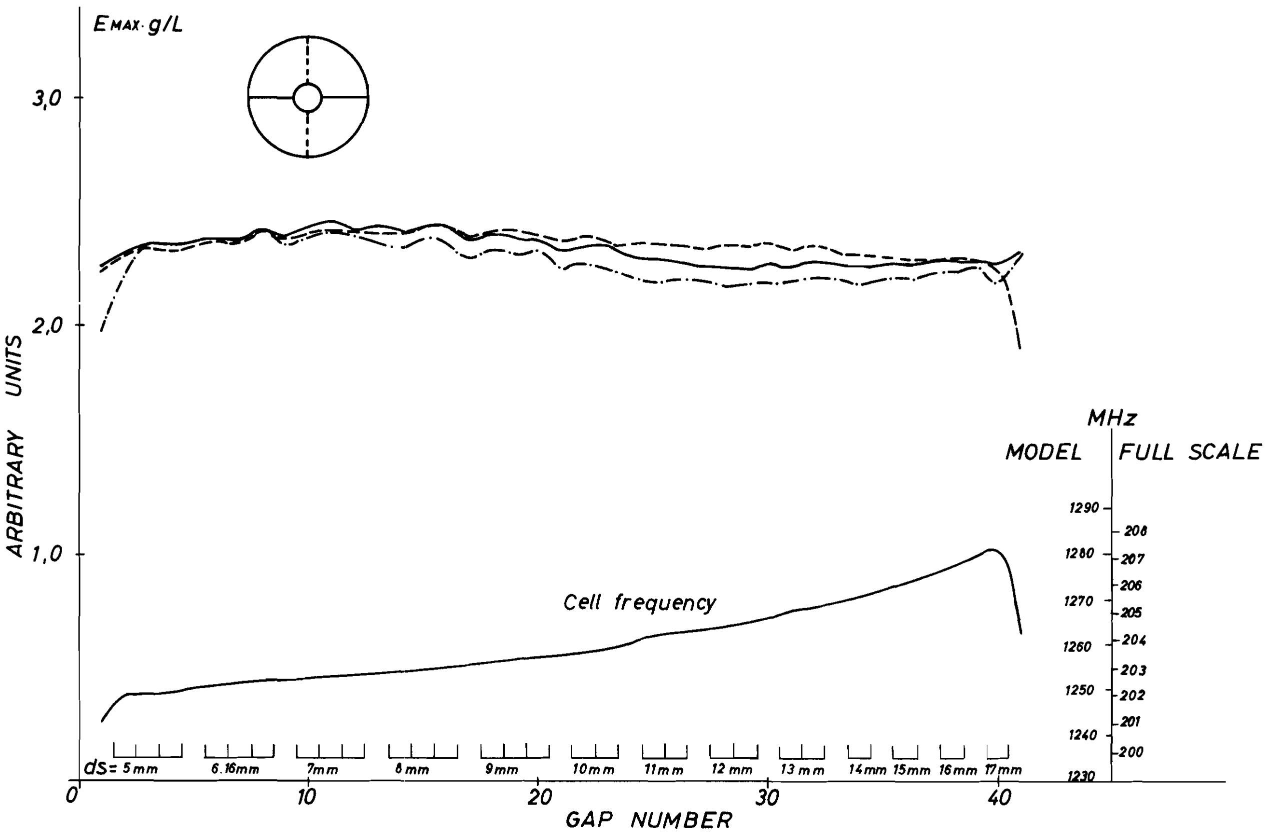

Fig. 16. Field stability against perturbation and resonant frequency of the individual cells in the Alvarez mode, for tank 2 model. Structure compensated locally, with experimental values of stem diameter d_s adjusted by trial and error.

——— without perturbation (frequency: 1255.99 MHz)
- - - with a tank perturbation of - 2 MHz in cell 41
-.-.-. with a tank perturbation of - 2 MHz in cell 1.

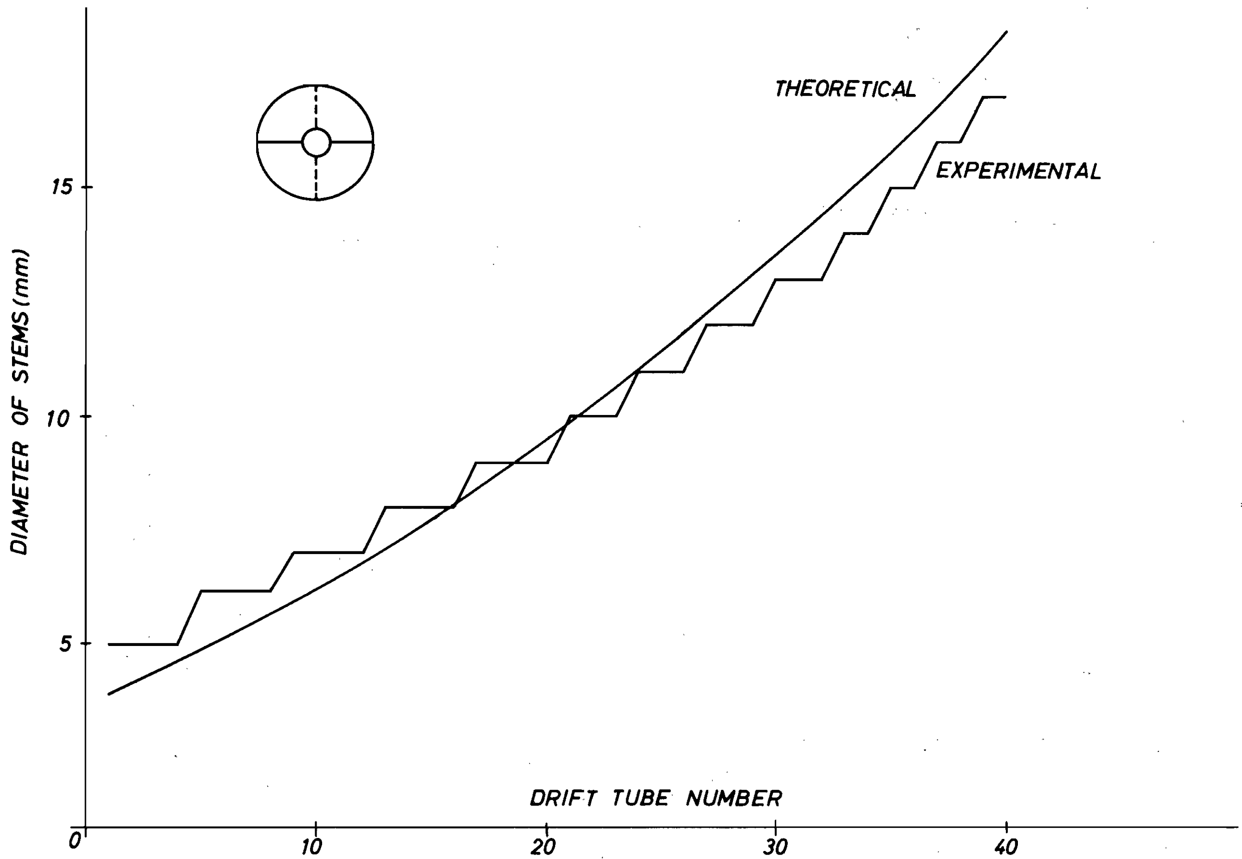

Fig. 17. Stem diameters for locally compensated cross-bar structure. A comparison between theoretical and experimental curves.

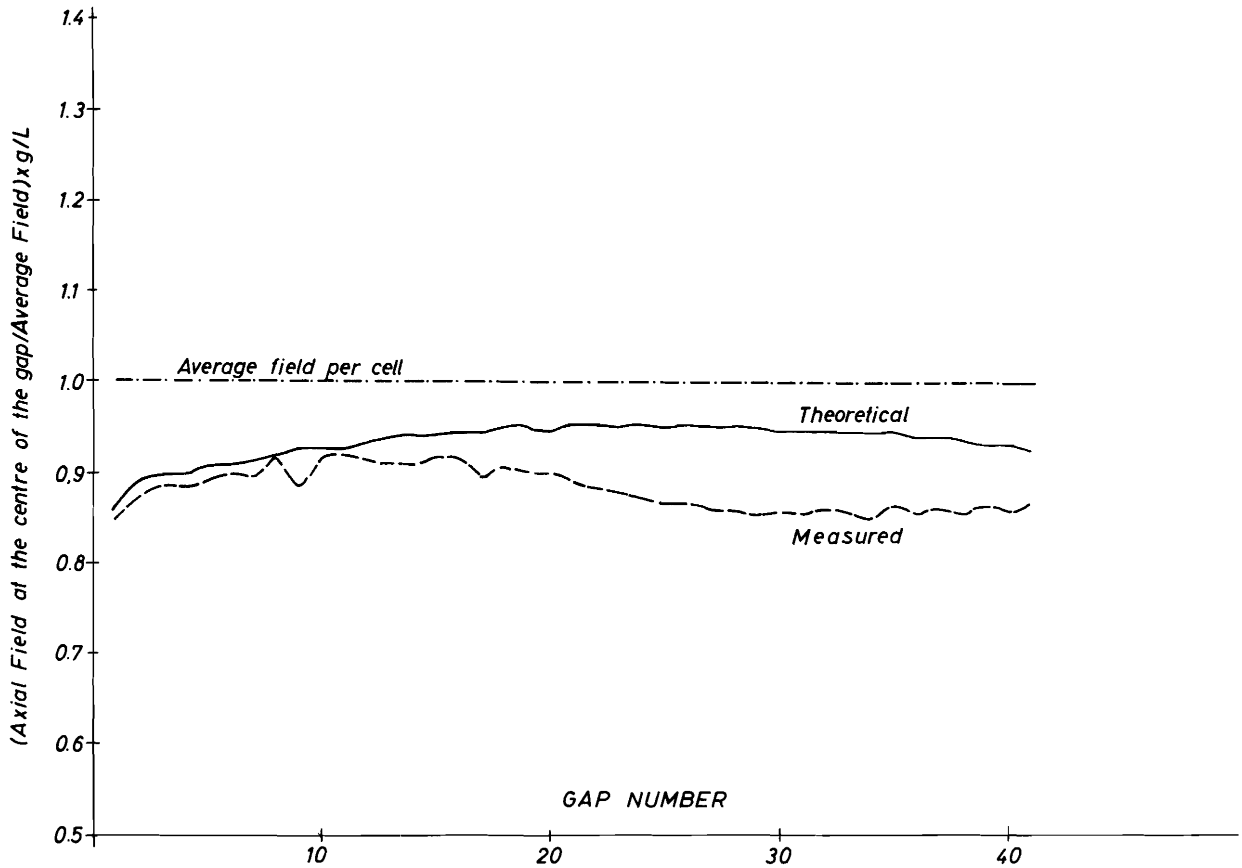

Fig. 18. Comparison of theoretical and measured electric field at the centre of the gaps, for the best locally compensated tank 2 model.

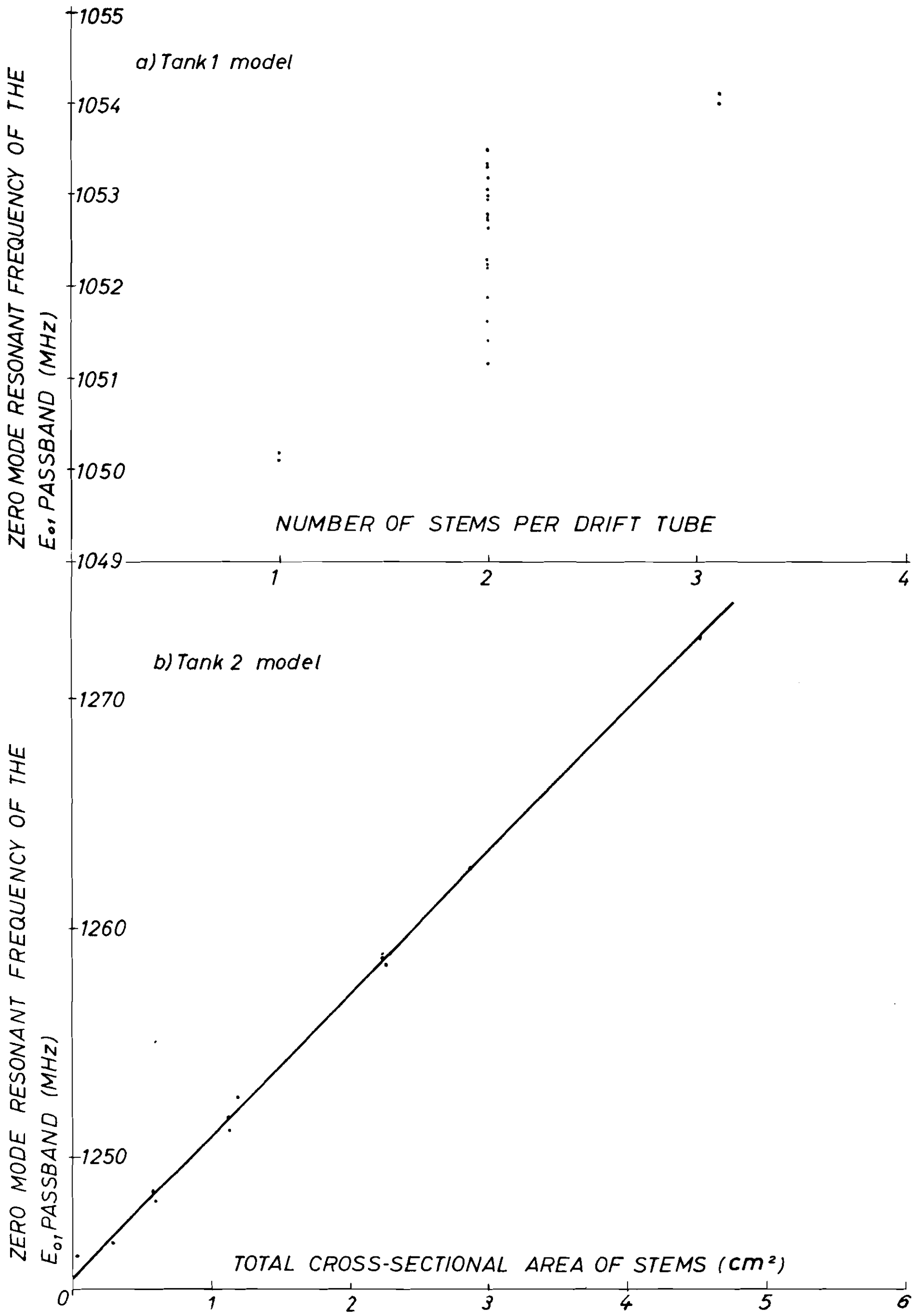

Fig. 19. Experimental frequency shift of the Alvarez 0 mode due to the stems.
a) Tank 1 model; b) Tank 2 model.